

Inhibition of Ricin by an RNA Stem–Loop Containing a Ribo–Oxocarbenium Mimic

Xiang-Yang Chen, Todd M. Link, and Vern L. Schramm*

Department of Biochemistry
Albert Einstein College of Medicine of
Yeshiva University, 1300 Morris Park Avenue
Bronx, New York 10461

Received January 4, 1996

Ricin is a cytotoxic heterodimeric protein isolated from castor beans.¹ It is one of the most toxic substances, with a single ricin molecule being lethal for eukaryotic cells.² Ricin's toxic nature is derived from its catalytic subunit, ricin toxin A-chain (RTA), which inactivates ribosomes and thereby destroys protein synthesis. Inactivation results from hydrolysis of a single *N*-ribosidic bond at adenosine 4324 in 28S rRNA.³ It is postulated that adenine depurination occurs through an oxocarbenium ion transition state (Figure 1), similar to that for AMP nucleosidase.⁴ The depurination site is located in a highly conserved stem–loop region, which has been established as a GA₄₃₂₄GA tetraloop.⁵ NMR structural studies indicate that stem–loop oligonucleotides with the GAGA tetraloop motif fold compactly in solution with an unusual base interaction between the first G and second A in the tetraloop. This G•A mismatch creates a sharp turn between the first G and first A in the phosphodiester backbone, exposing both the ribosyl moiety and the unpaired adenine base for catalytic attack by RTA.⁶ The GAGA tetraloop is essential for ricin enzymatic activity, while the sequence of the stem is only important to maintain stem–loop structure identity. However, RNA structures without stems have been shown to be poor substrates for RTA.⁷ The minimal substrate for ricin is reported to be an RNA 10-mer with the GAGA tetraloop.

It is of interest to obtain specific inhibitors of RTA due to its use in immunochemotherapy. Hydrolysis of the *N*-ribosidic bond of adenosine by nucleoside hydrolase from *Crithidia fasciculata* is chemically similar to that catalyzed by the RTA reaction.⁸ Nucleoside hydrolase stabilizes an oxocarbenium-ion transition state, characterized by protonation of the leaving group and distortion of the ribose toward the oxocarbenium.⁹ Phenyliminoribitol was synthesized as a transition state inhibitor of this enzyme and inhibits with a K_d of 30 nM.^{10,11} We proposed that ricin A-chain may also be subject to inhibition

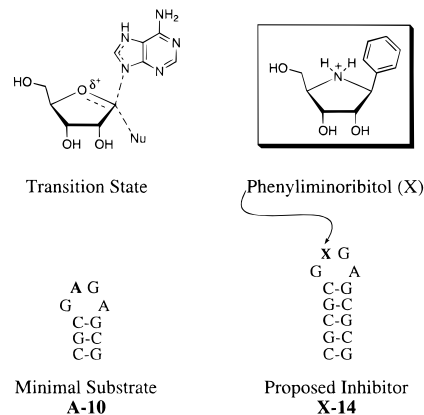


Figure 1. Proposed oxocarbenium-ion transition state of the ricin A-chain *N*-ribohydrolase reaction and a proposed inhibitor for incorporation into the site for depurination by ricin A-chain.

by phenyliminoribitol when placed in the suitable RNA context. In this communication, we report an approach to site-specific incorporation of phenyliminoribitol into stem–loop RNA at the RTA depurination site by chemical solid-phase RNA synthesis and describe its inhibitory properties.

Phenyliminoribitol (**1**, Scheme 1)¹¹ was protected by treatment with excess trifluoroacetic anhydride in dry pyridine, and subsequent *O*-hydrolysis in methanol containing two drops of concentrated ammonium hydroxide.¹² *N*-trifluoroacetylated **2** was protected with the dimethoxytrityl (DMT) group using DMTCl.¹³ Silylation of **3** with *tert*-butyldimethylsilyl chloride (TBDMSCl) gave a mixture of 2'- and 3'-silyl ethers in a ratio of 1:2, and attempts to improve the selectivity were unsuccessful.¹⁴ The desired 2'-silyl ether **4** was isolated by normal-phase HPLC (1% ethyl acetate in methylene chloride) or flash chromatography (methylene chloride:hexane = 8:1, R_f = 0.49 in CH₂Cl₂), and its structure was assigned by COSY NMR.¹⁵ Phosphitylation of **4** yielded crude phosphoramidite **5**.¹⁶ Without further purification, **5** was subsequently incorporated into the oligonucleotide, CGCGC GXGA CGCGC (**X-14**, Figure 1), by standard solid-phase RNA synthesis.¹⁷ Equivalent DMT release was observed during reactions of G, C, and **5**. The oligonucleotide was deprotected,¹⁷ purified by DEAE ion-exchange HPLC, eluting with 0–1.2 M ammonium acetate in 20% acetonitrile, and desalted on a G-10 Sephadex column in H₂O.¹⁸ The presence of phenyliminoribitol was verified by digesting **X-14** with snake venom phosphodiesterase and calf intestinal alkaline phosphatase followed by reversed-phase HPLC analysis. In addition, pXpG was synthesized according to the same procedure.²⁰

A synthetic oligonucleotide 10-mer (**A-10**, Figure 1) was synthesized as a RTA substrate. Samples were injected onto a

(12) (a) Sharma, R. A.; Bobek, M.; Bloch, A. *J. Org. Chem.* **1974**, *17*, 466–468. (b) The Fmoc group has also been used to block pyrrolidine nitrogen for solid-phase synthesis. See: Scharer, O. D.; Ortholand, J.-Y.; Ganesan, A.; Ezaz-Nikpay, K.; Verdine, G. L. *J. Am. Chem. Soc.* **1995**, *117*, 6623–6624.

(13) *Oligonucleotides and Analogues: A Practical Approach*; Eckstein, F., Ed.; IRL: Oxford, 1991.

(14) Hakimelahi, G. H.; Proba, Z. A.; Ogilvie, K. K. *Can. J. Chem.* **1982**, *60*, 1106–1113.

(15) Also see: Altmann, K.-H.; Freier, S. M.; Pieleas, U.; Winkler, T. *Angew. Chem., Int. Ed. Engl.* **1994**, *33*, 1654–1657.

(16) Scaringe, S. A.; Francklyn, C.; Usman, N. *Nucleic Acids Res.* **1990**, *18*, 5433–5441.

(17) *Protocols for Oligonucleotides and Analogs: Synthesis and Properties*; Agrawal, S., Ed.; Methods in Molecular Biology 20; Humana: New Jersey, 1993.

(18) Sproat, B.; Colonna, F.; Mullah, B.; Tsou, D.; Andrus, A.; Hampel, A.; Vinayak, R. *Nucleosides Nucleotides* **1995**, *14*, 255–273.

(19) Allerson, C. R.; Verdine, G. L. *Chem. Biol.* **1995**, *2*, 667–675.

(20) Phosphorylation of XpG was achieved by automated chemical synthesis. Electrospray mass spectrometry gave the expected m/z = 714.

* Author to whom correspondence should be addressed: telephone (718) 430-2813; FAX (718) 430-8565; email vern@aeom.yu.edu.

(1) (a) Olsnes, S.; Pihl, A. *Biochemistry* **1973**, *12*, 3121–3126. (b) Barbieri, L.; Battelli, M. G.; Stürpe, F. *Biochim. Biophys. Acta* **1993**, *1154*, 237–282.

(2) Olsnes, S.; Pihl, A. In *Molecular Action of Toxins and Viruses*; Cohen, P., van Heyningen, S., Eds.; Elsevier Biomedical: New York, 1982; pp 51–105.

(3) Endo, Y.; Tsurugi, K. *J. Biol. Chem.* **1987**, *262*, 8128–8130.

(4) (a) Mentch, F.; Parkin, D. W.; Schramm, V. L. *Biochemistry* **1987**, *26*, 921–930. (b) Lord, J. M.; Roberts, L. M.; Robertus, J. D. *FASEB J.* **1994**, *8*, 201–208.

(5) (a) Endo, Y.; Tsurugi, K. *J. Biol. Chem.* **1988**, *263*, 8735–8739. (b) Endo, Y.; Gluck, A.; Wool, I. G. *J. Mol. Biol.* **1991**, *221*, 193–207. (c) Gluck, A.; Endo, Y.; Wool, I. G. *Nucleic Acids Res.* **1994**, *22*, 321–324.

(6) (a) Szewczak, A. A.; Moore, P. B.; Chan, Y.-L.; Wool, I. G. *Proc. Natl. Acad. Sci. U.S.A.* **1993**, *90*, 9581–9585. (b) Orita, M.; Nishikawa, F.; Shimayama, T.; Taira, K.; Endo, Y.; Nishikawa, S. *Nucleic Acids Res.* **1993**, *21*, 5670–5678.

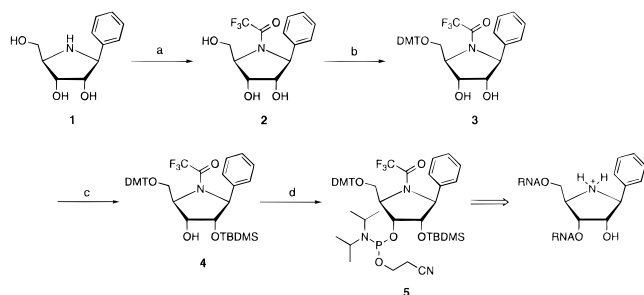
(7) Gluck, A.; Endo, Y.; Wool, I. G. *J. Mol. Biol.* **1992**, *226*, 411–424.

(8) Parkin, D. W.; Horenstein, B. A.; Abdulah, D. R.; Estupinan, B.; Schramm, V. L. *J. Biol. Chem.* **1991**, *266*, 20658–20665.

(9) Horenstein, B. A.; Parkin, D. W.; Estupinan, B.; Schramm, V. L. *Biochemistry* **1991**, *30*, 10788–10795.

(10) Horenstein, B. A.; Schramm, V. L. *Biochemistry* **1993**, *32*, 9917–9925.

(11) Horenstein, B. A.; Zabinski, R. F.; Schramm, V. L. *Tetrahedron Lett.* **1993**, *34*, 7213–7216.

Scheme 1^a

^a Conditions: (a) (i) $(\text{CF}_3\text{CO})_2\text{O}$, py; (ii) NH_4OH , MeOH, 84%; (b) DMTCl, Et_3N , DMAP, py, 81%; (c) TBDMSCl, AgClO_4 , py, THF, 31%; (d) 2-cyanoethyl *N,N*-diisopropylchlorophosphoramidite, 2,4,6-collidine, *N*-methylimidazole, CH_2Cl_2 .

reversed-phase C18 analytic column with isocratic elution in 50 mM ammonium acetate (pH 5.0) containing 10% methanol, at a flow rate of 1 mL/min. The adenine peak was compared to adenine standards treated in the same way. K_m and k_{cat} of stem-loop RNA **A-10** were determined to be $6.2 \pm 0.7 \mu\text{M}$ and $1.7 \pm 0.1 \text{ min}^{-1}$, respectively (Figure 2, upper), similar to those recently reported for a 19-base stem-loop RNA.¹⁹

Addition of the stem-loop **X-14** at $4 \mu\text{M}$ caused 75% inhibition of RTA using $10 \mu\text{M}$ **A-10** as substrate. The inhibition data (Figure 2, lower) gave a good fit to the expression $v = (k_{\text{cat}}A)/(K_m(1 + I/K_i) + A)$, which assumes that **A-10** and **X-14** compete for the catalytic site. The inhibition constant (K_i) is $0.73 \pm 0.02 \mu\text{M}$. Neither phenyliminoribitol (**X**) nor pXpGp exhibited significant inhibition at concentrations of 200 and $100 \mu\text{M}$, respectively. Thus, the inhibitor is most efficient in the stem-loop structure.

The mechanism of action of RTA hydrolysis has been proposed by X-ray crystal structural analysis.^{21ab} In the crystal structure, the adenine ring π -stacks between tyrosines 80 and 123, while the proposed oxocarbenium ion could be stabilized by ion pairing to Glu 177. When phenyliminoribitol is positioned at the targeted adenosine site, it would fit into the proposed structure by hydrogen bonding between nitrogen on the azasugar ring with Glu 177 and π -stacking of phenyl ring between Tyr 80 and 123 at the RTA active site, similar to the interactions proposed for **1** with nucleoside hydrolase.²² Therefore, good binding is achieved between **X-14** and RTA.

Although the binding of **X-14** to RTA is 10-fold better than for the substrate, it is weaker than expected for an efficient transition state inhibitor.²³ Leaving-group interactions are known to be important in considering transition state interactions of related *N*-ribohydrolases²⁴ and will need to be considered in improved inhibitor design for RTA.

(21) (a) Monzingo, A. F.; Robertus, J. D. *J. Mol. Biol.* **1992**, *227*, 1136–1145. (b) Weston, S. A.; Tucker, A. D.; Thatcher, D. R.; Derbyshire, D. J.; Paupit, R. A. *J. Mol. Biol.* **1994**, *244*, 410–422.

(22) Parkin, D. W.; Schramm, V. L. *Biochemistry* **1995**, *34*, 13961–13966.

(23) Schramm, V. L.; Horenstein, B. A.; Kline, P. C. *J. Biol. Chem.* **1994**, *269*, 18259–18262.

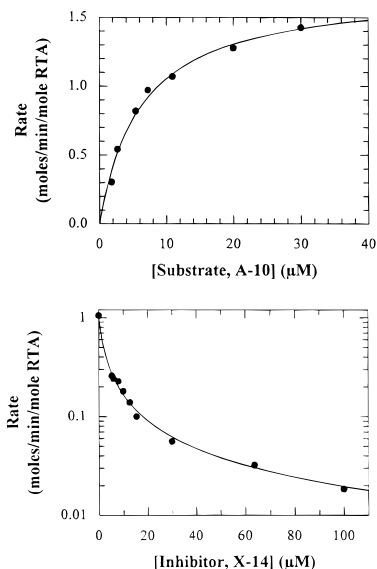


Figure 2. Substrate saturation of RTA by **A-10** (upper panel). Reactions were in $50 \mu\text{L}$ of buffer (10 mM KCl, 1 mM EDTA, and 10 mM Tris-HCl (pH 7.5)) containing $0.2 \mu\text{M}$ RTA and the indicated concentrations of **A-10**. After incubation at 37°C for 10 min, the released adenine was analyzed by HPLC. The rate of adenine release was linear with time to approximately 30 min. The line was drawn from a fit of the experimental data to the equation for a rectangular hyperbola to obtain values of K_m and k_{cat} . The lower panel shows the inhibition of RTA by **X-14** using $10 \mu\text{M}$ stem-loop **A-10** as substrate. Reactions were in $50 \mu\text{L}$ of the same buffer containing $1.2 \mu\text{M}$ RTA, $10 \mu\text{M}$ **A-10**, and the indicated concentrations of **X-14**. After incubation at 37°C for 30 min, the released adenine was analyzed by HPLC. The line is the best fit of the data to the equation for competitive inhibition (see text).

In summary, we have incorporated a purine *N*-glycohydrolase inhibitor into stem-loop RNA and developed a convenient assay for screening inhibitors with RTA. Stem loop RNA with an oxocarbenium-ion mimic at the RTA depurination site exhibits promising submicromolar inhibition activity for the hydrolytic action of RTA. Further study of the RTA depurination mechanism is being conducted to develop the next generation of inhibitors for ricin and its potential chemotherapeutic applications.

Acknowledgment. This work was supported by the U.S. Army Medical Research and Development Command under Contract No. DAMD 17-93-C-3051. The views, opinions, and/or findings contained in this report are those of the authors and should not be construed as an official Department of the Army position, policy, or decision unless so designated by other documentation. The authors thank Dr. Jon Robertus, University of Texas, Austin, for the generous supply of ricin A-chain.

JA9600385

(24) Mazzella, L. J.; Parkin, D. W.; Tyler, P. C.; Furneaux, R. H.; Schramm, V. L. *J. Am. Chem. Soc.*, in press.